Morphology Behavior of Polysulfone Membranes Made from Sustainable Solvents

Steven Kluge *, Karla Hartenauer , Murat Tutuş

Posted Date: 30 April 2024

doi: 10.20944/preprints202404.2010.v1

Keywords: polysulfone; membranes; sustainable solvents; gas separation; biogas; morphology; gas separation membranes; REACh

 doi:10.20944/preprints202404.2010.v1

Article

Morphology Behavior of Polysulfone Membranes Made from Sustainable Solvents

Steven Kluge [1,*], Karla Hartenauer [1] and Murat Tutuş [1]

Fraunhofer-Institute for Applied Polymer Research IAP
* Correspondence: steven.kluge@iap.fraunhofer.de; Tel.: +49 331 5681224, SK

Abstract: In a previous study we could show a change of membrane morphology and gas separation performance by varying the recipe of a casting solution based on polysulfone in a determined solvent system. Although all results were very reproducible, all used solvents were harmful and not sustainable. In this study therefore, the solvents tetrahydrofuran (THF) and N,N-dimethylacetamide (DMAc) are replaced by the more sustainable solvents 2-methyl-tetrahydrofuran (2M-THF), N-butyl pyrrolidinone (NBP) and cyclopentyl methyl ether (CPME). The gas permeation performance and for the first time morphology of the membranes before and after solvent replacement were determined and compared by single gas permeation measurements and SEM microscopy. It is shown, that THF can be replaced by 2M-THF and NBP without decreasing the gas permeation performance. With CPME replacing THF no membranes were formed. Best gas permeation results showed systems with 2M-THF as THF alternative. Permeances for the tested gases oxygen (O_2), nitrogen (N_2), carbon dioxide (CO_2) and methane (CH_4) were $2.66 \cdot 10^{-4}$, $3.89 \cdot 10^{-5}$, $1.53 \cdot 10^{-3}$ and $4.52 \cdot 10^{-5}$ mL(STP)/cm²·min·bar, respectively. permselectivities of those membranes for the gas pairs O_2/N_2, CO_2/N_2 and CO_2/CH_4 were 6.7, 38.3 and 34.0, respectively. When additionally replacing DMAc in the solvent system no or only porous membranes were obtained, even if the precipitation procedure was adjusted. These findings indicate that a complete replacement of the solvent system without affecting the membrane morphology or gas permeation performance is not possible. By varying the temperature of the precipitation bath an easy adjustment to mechanically stable PSU membranes is possible, if just THF was replaced by 2M-THF.

Keywords: polysulfone; membranes; sustainable solvents; gas separation; biogas; morphology; gas separation membranes; REACh

1. Introduction

Against the background of environmental and climate problems, a new field of work is opening for work in chemistry and especially with polymer materials in the 21st century. The use of recently used solvents is not sustainable. In the interests of developing more environmentally friendly and more sustainable processes and products, alternatives to conventional solvents are increasingly being implemented and optimized. This topic also affects the research area of polymeric membranes. In particular those, based on polymer solutions.

For non-solvent induced phase separation (NIPS), which is the most versatile method, traditionally tetrahydrofuran (THF), N,N-dimethyl acetamide (DMAc) as well as N,N-dimethyl formamide (DMF) and N-methyl-2-pyrrolidone (NMP) are used [1–6].Besides disposal a dangerous risk to humans is given. Additionally, the risk of long-term problems regarding human health and environmental pollution is growing [7,8]. The European Chemical Agency (ECHA) will also restrict on industrial use of NMP, DMAc and DMF [9].

Over 90 % of industrial waste is accounted for wastewater contamination by solvents used in membrane fabrication which is about 20-100 billion liters annually [10–12]. Recycling of the wastewater is desirable but not always applicable because of requirements regarding purity and regulations [13,14]. Based on the 3Rs for circular economy, reduce, reuse and recycle, reuse is no option, since waste from membrane fabrication must be treated. Therefore, reduce and recycle are applicable, where reduce should be the most favorable option [15,16]. To overcome these the

 doi:10.20944/preprints202404.2010.v1

challenges with often used harmful solvents the use of more sustainable solvents is an appropriate alternative.

The research on more sustainable membrane materials and solvents is a growing field [13,17–21]. Recent research in the field of sustainable solvents deals with Rhodiasolv PolarClean [8,22–24], Cyrene [8], dimethyl sulfoxide (DMSO) [25–27], γ-valerolactone (GVL) [28] dimethyl isosorbide (DMI) [12] and NBP [29,30]. Moreover, toxicity and hazardousness are just two aspects that have to be taken into consideration for more sustainable solvents. More aspects like energy required to produce alternative solvents and the potential of recycling or disposal also must be considered [31].

The aforementioned NIPS process uses in general three components. These are the polymer, a solvent and a non-solvent. The solvent is able to bring the polymer in solution to have a polymer solution which is able to make a defect free wet film (protomembrane) on a support. By putting the protomembrane in a non-solvent bath, the miscibility gap of the solvent-polymer system is reached, resulting in phase separation. In this case liquid-liquid demixing occurs and a polymer-poor and a polymer-rich phase is formed within the protomembrane. The polymer-poor phase causes large finger-like or drop-shaped voids or smaller bubble-shaped voids [32,33]. The resulting membrane morphology can be estimated by solubility parameters of the polymer, the solvent and non-solvent. These estimations are built on assumptions and practical experience which are based on empirical and physicochemical data [30]. Parameters for tuning the membranes morphology are for example the composition of the casting solution, the precipitation medium, temperature of the precipitation bath and residence times [1,33–39].

Water is very often used as a non-solvent, because most polymers are soluble in water miscible solvents but not in water. For the NIPS process organic solvents need to be completely miscible with water. The small and polar water molecules are diffusing one to two orders of magnitude faster from the precipitation bath into the protomembrane, compared to organic solvents diffusing from the protomembrane into the precipitation bath, which is often resulting in large voids causing a mechanically less stable membrane [36].

If all parameters are controlled to have a dense gas separation layer in a membrane the latter can used for gas separation. Gas separation is based on different permeation behavior of different gases in a membrane. Permeation of gases in a membrane can be described in two steps. Firstly, the sorption of gases into the membrane is required [40]. Just if this step has taken place the second step, namely diffusion, can happen due to an external driving force [41–44]. The driving force is a difference in the chemical potential between the feed and the permeate site of a membrane. The chemical potential in gas separation is applied via a pressure difference.

The aim of this study is additionally to studies about the use of more sustainable solvents to control the morphology of resulting membranes. Since all solvents have different solubility parameters and therefore affecting the membrane morphology, this study for the first time shows that even with more sustainable solvents it is possible to come to mechanically stable gas separation membranes. Furthermore, this study shows that control of the resulting membrane morphology is still possible independently, from the fact that sustainable solvents show other solution behavior compared to traditional, harmful solvents for membrane fabrication.

2. Materials and Methods

In this section, materials and methods used for this study are listed and explained to give readers or interested people the opportunity to reproduce our experiments.

2.1. Materials

Polysulfone, P-3500 LCD MB7 (78.6 kg/mol, Solvay), was used to fabricate PSU flat sheet membranes. Polydimethylsiloxane (Elastosil RT 625 A and B, PDMS, Wacker Chemie AG) was used to coat the fabricated polysulfone membranes. Tetrahydrofuran (99.9 %; Roth), N,N-dimethyl acetamide (99.5 %; Roth), methanol (99.9 %; Roth), ethanol (99.5 %; Roth) and n-heptane (≥ 95 %; Roth) were used as-received.

 doi:10.20944/preprints202404.2010.v1

2.2. Membrane Preparation

The desired amount of solvent was filled into a capped flask and PSU pellets were added. Polysulfone and solvents were mixed in the closed flask for 16 h on a roller bench until a homogenous, yellowish polymer solution was obtained. In order to shift the solubility equilibrium closer to the demixing point, a certain mass of methanol was then added to the polymer solution drop by drop and further mixed until the solution was homogenous again. The obtained casting solution was then poured onto a glass plate and fabricated to a polymer film with the aid of a casting knife set to 250 µm gap height at a speed of 17 mm/s (1 m/s). The glass plate was immediately after casting immersed in the precipitation bath for thirty minutes. To wash away remaining solvents the precipitated membranes were rinsed with distilled water for about one minute on each side. Afterwards the washed membranes were left to dry at room temperature in a dust free box for at least 16 hours. If applied, PSU membranes were coated with PDMS (9:1 = component A:component B, 70 % by mass in n-heptane) after they had dried.

2.3. Determination of Membrane Thickness

The magnetic inductive method is a type of non-destructive material testing to analyze the thickness d of electrically insulating materials or coatings on ferromagnetic substrates. For this purpose, the non-magnetic material – in this case a polymer membrane – is placed on a steel plate and measured at several points. The probe consists of an iron core wrapped with a measuring coil and an excitation coil to which a low-frequency alternating current is applied, which creates an alternating magnetic field around the iron core.

If the probe approaches the material and thus also the ferromagnetic base during the measurement, the magnetic field increases. Depending on the distance or the layer thickness of the non-magnetic material, a voltage is detected by the measuring coil. This voltage is proportional to the thickness of the non-magnetic material. The gained voltage is evaluated digitally. The morphology of membranes is not considered in these kinds of measurements. The measuring principle is shown in Figure 1.

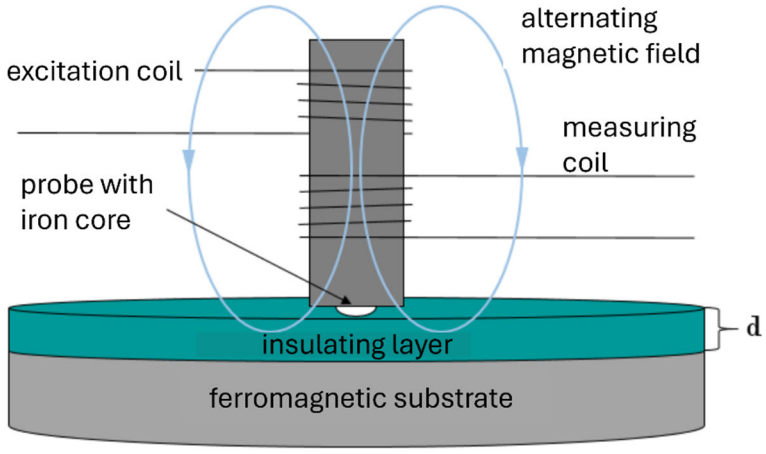

Figure 1. Measuring principle of magnetic inductive layer thickness measurement.

In this work, a device from Helmut FISCHER from the FMP 10-20 series with a stainless-steel plate as a ferro-magnetic base was used. This device measures the composite of PSU and PDMS, as well as both components individually. Since the membranes rarely have a smooth surface, even slight unevenness could lead to different measurement results. To check this measurement inaccuracy, the layer thickness is also measured optically in a scanning electron microscope.

2.4. Scanning Electron Microscopy

To examine the membrane structures obtained, scanning electron micrographs were taken with an EVO 15 SmartSEM (Carl Zeiss NTS, Germany). For this purpose, the samples were immersed in

 doi:10.20944/preprints202404.2010.v1

liquid nitrogen, broken and were then applied to a conductive carrier before they were vapor-deposited with a 4 nm thick layer of gold. The samples have been measured at an acceleration voltage of 9.46 – 20.00 kV. The SEM images in this paper only include membrane samples from polysulfone membranes without a PDMS protective layer, since the focus of this work is on PSU flat sheet membranes.

2.5. Gas Permeation Measurements

Gas permeation tests were conducted using a time-lag apparatus. Permeabilities of the coated membranes for oxygen (O2), nitrogen (N2), methane (CH4) and carbon dioxide (CO2) were determined using the time-lag method at 25 °C. The measurements were performed after an evacuation duration of 1.5 hours after every sample exchange and of twelve time-lags (Θ) in between the measurements (minimum 3 min, maximum 6 h). To minimize measurement uncertainties, each gas was measured twice and at different feed pressures of 390 mmHg (520 mbar) and 600 mmHg (800 mbar). The permeate pressure was set to 7.5 · 10-5 mmHg (1 · 10-4 mbar) at the beginning of each measurement [45].

The apparatus measures the time-dependent pressure increase of the permeate to obtain a time-pressure curve for every gas. A schematic representation of such a curve is given in Figure 2.

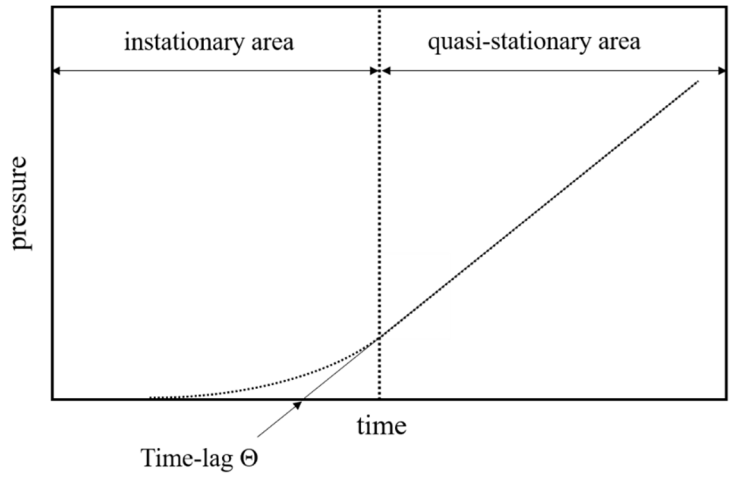

Figure 2. Exemplary depiction of a time-pressure curve obtained from the time-lag measurement.

From the time-lag measurements, two properties can be determined: the permeability P_i and the diffusion coefficient D_i of gas i. The gas permeability P_i is calculated as follows:

$$P = \frac{l \cdot V(\mathrm{STP})}{A \cdot t \cdot (\Delta p_\mathrm{F} - \Delta p_\mathrm{P})} \quad (1)$$

where l is the membrane thickness [cm], $V(\mathrm{STP})$is the volume of the permeate [cm³], A is the effective membrane area [cm²], t the passed time within the quasi-stationary range [s], Δp_F: the difference of the feed pressure within the quasi-stationary range [cmHg]and Δp_P the difference of the permeate pressure within the quasi-stationary range [cmHg]. Permeabilities are given in Barrer (1 Barrer = 10^{-10} $\frac{\mathrm{cm^3(STP)\cdot cm}}{\mathrm{cm^2\cdot s\cdot cmHg}}$).

Diffusivities D_I of a certain gas i can be calculated from the time lag Θ according to the following equation:

$$\mathrm{D} = \frac{l^2}{6\Theta} \quad (2)$$

The time lag Θ is determined graphically from the time-pressure diagrams by extrapolating the linear range of the pressure increase to the time axis (Figure 2).

 doi:10.20944/preprints202404.2010.v1

The permeability selectivity (permselectivity) $\alpha_{A,B}$ of a membrane in relation to two gases A and B is also called ideal selectivity and is determined according to Eq. 5 from the ratio of the permeabilities of gases A and B within the linear range of the pressure increase.

$$\alpha_{A,B} = \frac{P_A}{P_B} \quad (3)$$

Another measure for a membrane's performance is the ability to separate a gas mixture. In this case, a separation factor is obtained according to Eq. 6, where xi is the concentration of gas i in the feed and yi is the concentration of gas i in the permeate.

$$\mathbb{A}^*_{A,B} = \frac{y_A/y_B}{x_A/x_B} \quad (4)$$

The separation factor typically exhibits lower values than the permselectivity due to effects such as plasticization of the membrane material caused by molecules like e.g. water or CO2. With the gas permeation setup at Fraunhofer IAP, it is possible to determine permselectivities.

The solubility can be calculated as the ratio of permeability and diffusivity according to the following equation:

$$S = \frac{D}{P} \quad (5)$$

In the present work, solubility has no independent significance and is only mentioned demonstratively.

3. Results and Discussion

Membranes reported elsewhere [33] and their morphology revealed a gas separation layer of around 20 to 50 nm and a sponge-like support structure. This membrane structure is favorable in gas separation applications at elevated pressures. The composition of the casting solution of these membranes is given in Table 1.

Table 1. Compositions of membranes with harmful solvents [33].

Condition	Value and unit
Composition of the casting solution	25 wt-% PSU 58.28wt-% THF 3.72 wt-% DMAc 13 wt-% MeOH
Gap height of casting knife	250 µm
Casting speed	17 mm/s
Free standing duration	≈3 s
Precipitation medium	Water for 4 min
Washing step	60 s under running water (top and bottom side each)
Drying step	16 h in fume hood
Lab temperature	21 °C
Post treatment	Coating with PDMS-layer after drying @ RT

Membranes formed within conditions listed in Table 1 showed the following mechanically stable morphology (Figure 3). This morphology shows a very thin separation layer and a sponge-like support structure beneath the separation layer. The thickness of the overall membrane lies in the range of 90 – 110 µm.

 doi:10.20944/preprints202404.2010.v1

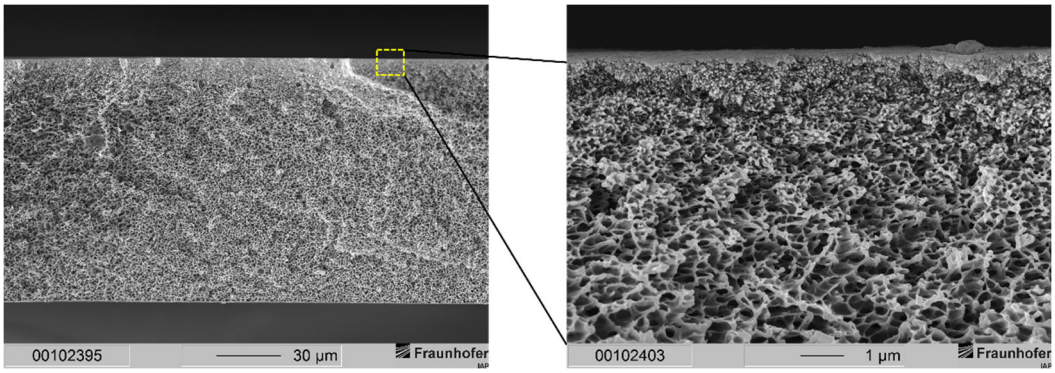

Figure 3. Left: Cross section of a non-layered PSU flat sheet membrane fabricated according to conditions shown in Table 1. Right: Enlarged view of the top layer with dense separation layer and sponge like support structure.

However, the solvents used in this publication are listed as toxic and harmful to the environment [2,7,8]. As there are greener alternatives, it is known that different solvents show different solubility parameters [8]. These parameters are affecting the resulting membrane structure during precipitation leading to different mechanical stability and even differing gas separation performance [33,37]. Even the size of the solvent molecules is reported to have influence on the resulting gas separation performance of the membranes [46].

3.1. Solvent Exchange

The solvent system of membranes listed in Table 1 consists of two solvents and one co-solvent. Since the latter has a completely different effect on the solution and therefore for the resulting membrane, only the two solvents, namely THF and DMAc, are exchanged in this study. Methanol therefore remains part of all test systems. An exchange of methanol must be investigated in further research in this field.

As an alternative for THF and DMAc three more sustainable solvents were provided:

- N-Butyl-2pyrrolidinone (NBP)
- 2-Methyl-Tetrahydrofurane (2M-THF)
- Cyclopentyl methyl ether (CPME)

These solvents shall be used as both THF and DMAc replacements. The amounts are not changed due to directly observe changes in morphology of the resulting membranes.

3.1.1. Replacement of THF

In a first step THF was replaced by NBP, 2M-THF and CPME. This results in the solvent systems shown in Table 2.

Table 2. Solvent systems in which the main solvent THF is replaced.

Solvent system	Solvent 1	Solvent 2
M1	NBP	DMAc
M2	2M-THF	DMAc
M3	CPME	DMAc

After preparation, processing and characterization of all solvent systems shown in Table 2, all that result in functional membranes are also subject to replacement of DMAc in a next step of solvent exchange.

 doi:10.20944/preprints202404.2010.v1

3.1.2. Replacement of DMAc

After THF replacement is tested, DMAc is replaced. The working THF alternatives continue to be used for this step. Table 3 shows all tested solvents in which THF, **and** DMAc are replaced.

Table 3. Solvent Systems with working THF alternatives in which DMAc is replaced additionally.

Solvent system	Solvent 1	Solvent 2
M4	NBP	2M-THF
M5	NBP	CPME
M6	2M-THF	NBP
M7	2M-THF	CPME

After all solvent tests have been completed, a solvent system is selected to vary parameters in membrane forming. i.e. temperature of the precipitation bath. This decision is based on the properties of the membranes of these solvent systems. The evaluation criteria are:

- gas permeance
- stability
- morphology
- sustainability

Whereby the former is the most important and decisive factor, as it affects the separation performance of the membranes. Stability and morphology can possibly be achieved by changing the composition of the solution or process parameters in membrane formation. In case of several equal solvent systems, the solvents used per system are compared in terms of sustainability and the more sustainable system is selected.

3.1.3. Variation of Temperature of the Precipitation Bath

In this series of experiments, the temperature of the precipitation bath, which is used in the standard process at room temperature, is changed. Membranes are prepared at precipitation bath temperatures of 0 °C and 60 °C. These values were chosen to cover the temperature range between the freezing point of the precipitation medium and the evaporation temperature of the co-solvent methanol.

Diffusion in liquids is described by the Stokes-Einstein-Equation:

$$D = \frac{k_B T}{6\pi\eta r} \tag{6}$$

Equation (6) shows that the diffusion coefficient D depends on the temperature T of the environment, the viscosity η and, assuming that the particles are spherical, on the radius r of these particles. The Boltzmann constant k_B ($1.38 \cdot 10^{-23} \frac{J}{K}$) is the conversion factor for absolute temperature in relation to absolute, physical zero in energy. It should also be noted that this connection is independent of the charge of the diffusing particles and a proportionality of the friction force to the molecular speed is assumed.

According to equation (6), it can be assumed that the temperature of the precipitation bath influences the diffusion of the solvent and the precipitation medium and thus also the morphology of the resulting membranes. As the temperature increases, the rate of diffusion increases, while it would decrease at lower temperatures.

By reducing the precipitation bath temperature, a more homogeneous, stable membrane morphology can be expected. To experience the full effect of precipitation bath temperature, it is also increased, although a less favorable morphology is expected.

 doi:10.20944/preprints202404.2010.v1

3.2. Gas Permeation Measurements

To characterize gas separation properties of all fabricated membranes, single gas permeation measurements were conducted. The permeability of a membrane is hard to determine since the thickness of the selective layer is varying over the hole membrane area. On the other hand, the thickness is varying from membrane to membrane. Additionally, as we showed in our previous paper, the permeability is strongly dependent on the chain arrangement of the polymer inside the membrane. Therefore, in this paper permeation behavior of the membranes is expressed as permeance, which is independent of the thickness of the gas separating layer or membrane in general.

3.2.1. Replacement of THF

Having a starting point to compare the membrane performance, a standard membrane made from THF, DMAc and MeOH (see Table 1) was prepared and studied. The resulting permeances and permselectivities are shown in Tables 4 and 5.

Table 4. Permeances from the standard PSU-membrane made from the solvent system THF, DMAc and MeOH.

Permeance [mL(STP)/(cm²·min·bar)]			
O_2	N_2	CO_2	CH_4
$2.87 \cdot 10^{-4}$	$4.1 \cdot 10^{-5}$	$1.63 \cdot 10^{-3}$	$5.75 \cdot 10^{-5}$

Table 5. Permselectivities for the standard PSU-membrane made from the solvent system THF, DMAc and MeOH.

O_2/N_2	**CO_2/N_2**	**CO_2/CH_4**
7.0	39.8	32.5

Membranes prepared with NBP as solvent showed insufficient stability after four minutes of precipitation. Within this time, too less solvent is exchanged which lead to redissolution of the membranes whilst drying. During precipitation the membranes changed from transparent to white. In the redissolution step membranes changed back from white to transparent and they were getting softer compared to directly after precipitation. This is because water from the precipitation bath evaporates faster than NBP in the drying step and therefore a redissolution takes place. Water has a boiling point of 100 °C and NBP has a boiling point of 240.6 °C, resulting in faster evaporation of water compared to NBP causing redissolution.

To overcome this issue, the precipitation time was adjusted to 20 minutes. After this period the solvent was replaced by water in a manner that no redissolution occurred and all membranes could be left to dry. When 2M-THF was used as a THF alternative the effect of getting a transparent membrane again was not observed, after a precipitation time of 20 minutes. However, even if 20 minutes of precipitation time was not necessary for membranes prepared from 2M-THF it was still applicated to have similar membrane treatment and therefore better comparison between membranes prepared from those two solvents as THF alternative.

Results of membranes made from NBP and 2M-THF as THF alternative are listed in Tables 6 and 7.

Table 6. Permeances after THF replacement.

Solvent system	**Permeance** [mL(STP)/cm²·min·bar)]			
	O_2	N_2	CO_2	CH_4
M1	$2.18 \cdot 10^{-4}$	$3.95 \cdot 10^{-5}$	$1.25 \cdot 10^{-3}$	$4.92 \cdot 10^{-5}$
M2	$2.66 \cdot 10^{-4}$	$3.98 \cdot 10^{-5}$	$1.53 \cdot 10^{-3}$	$4.52 \cdot 10^{-5}$

 doi:10.20944/preprints202404.2010.v1

Table 7. Permselectivity after THF replacement.

Solvent system	O_2/N_2	CO_2/N_2	CO_2/CH_4
M1	5.7	32.7	28.8
M2	6.7	38.3	34.0

In comparison, the permeances shown in Table 6 are quite similar to each other and to the permeances of the standard membrane made from THF (Table 4). All permeances lie in the same order of magnitude. On the other hand, oxygen and carbon dioxide permeances were higher in 2M-THF-membranes compared to NBP-membranes. Nitrogen showed the same permeance within the uncertainty of measurement. Methane, on the other hand, showed a lower permeance in membranes prepared from 2M-THF. The difference of methane permeances in NBP- and 2M-THF-membranes should be treated with caution, since the uncertainty of measurement for the gas permeation machine has almost been reached at such low values. The uncertainty of measurement for our setup lies at $1.0 \cdot 10^{-5}$ mL/(STP)/cm²·min·bar. However, the changes of permeances of oxygen and carbon dioxide are significant.

Obviously, permselectivities for all gas pairs are smaller in NBP-membranes. The decrease is 15 - 20 % compared to THF- and 2M-THF-membranes. These values indicate pinholes in NBP-membranes. Those pinholes are closed by the PDMS-coating. Since this coating shows clearly lower permselectivities for all gas pairs, the result is a mixture of permselectivities of the PSU-membrane and a small area where just the PDMS-coating is the barrier between feed and permeate room. Therefore, the overall permselectivities in NBP-membranes are lower. Merkel et al. showed permselectivities for O_2/N_2, CO_2/N_2 and CO_2/CH_4 of 2.0, 7.0 and 3.2 at 35 °C, respectively [47].

The fact that permeances of NBP-membranes are slightly higher than those of 2M-THF-membranes indicates that the area of defects is very low but still affecting the separation performance.

However, as seen in picture 4 the membrane structure of membranes prepared from NBP and 2M-THF is different to membranes prepared from THF.

Membranes prepared from NBP and 2M-THF show a thin gas separation layer and large voids in their supporting structure. It can be seen that NBP-membranes lead to a more finger-like structure whereas 2M-THF-membranes show a drop-like shape of the voids.

In any case those void filled support structures are leading to less mechanically stable membranes. Voids are additionally an indicator for fast solvent exchange [48]. Especially, water is entering the wet protomembrane faster than solvents can enter the precipitation bath during precipitation. The osmotic pressure of water can reach up to 100 bar during precipitation. This is why water pushes polymer solution aside when penetrating the protomembrane. With ongoing precipitation, the polymer rich phase is solidifying resulting in thin walls building the void filled supporting structure of the membrane [36,48].

3.2.2. Replacement of DMAc

After replacing THF, the aim was replacing DMAc as well with a greener alternative. Even though CPME could not dissolve PSU when replacing THF, it was considered for a DMAc replacement because DMAc has a lower content of 15 wt-% in the solvent system than THF at 60 wt-%. Moreover, the aim of this study is to find a more sustainable solvent system. And CPME clearly is a more sustainable solvent than DMAc.

Firstly, THF was replaced again with NBP. In two separate approaches, DMAc was replaced once with 2M-THF and once with CPME. THF was then replaced with 2M-THF and additionally DMAc was replaced with NBP and then with CPME, separately. No analyzable membranes could be produced in either solvent system with 2M-THF as a THF replacement. When DMAc was replaced with CPME, PSU did not dissolve even after an extended period, preventing membranes from being fabricated. When DMAc is replaced by NBP, a solution is obtained, but after precipitation and drying the membrane is riddled with macroscopic defects in a way that no evaluable samples were obtained.

 doi:10.20944/preprints202404.2010.v1

The membranes in which THF was replaced by NBP required longer times for the polymer to dissolve. Usually twice as high as with any aforementioned membranes. The time required for precipitation was again 20 minutes. As a result, analyzable membranes were obtained.

When coating membranes prepared from NBP and 2M-THF with PDMS it was found that those membranes changed from white to transparent again. In addition, it was impossible to remove such membranes without defects from the surface on which they were manufactured. Even longer precipitation times or thermal treatment before coating could not completely solve the problem, because all membranes then formed macroscopic defects. Even though PSU membranes could not be coated, membranes prepared from NBP and 2M-THF as THF and DMAc alternatives were measured in gas permeation experiments. Using NBP and CPME this phenomenon was not observed. Those membranes were coated with PDMS as explained before. Results of membranes where both solvents, THF and DMAc were replaced are listed in Tables 8 and 9.

Table 8. Permeances after solvent exchange of both, THF and DMAc.

NBP as THF alternative				
Solvent System	**Permeance** [mL(STP)/cm²·min·bar)]			
2M-THF	O_2	N_2	CO_2	CH_4
	1.15	1.23	1.06	1.64
CPME	$2.92 \cdot 10^{-4}$	$1.41 \cdot 10^{-4}$	$1.33 \cdot 10^{-3}$	$2.17 \cdot 10^{-4}$

Table 9. Permselectivity after solvent exchange of both, THF and DMAc.

NBP as THF alternative			
Solvent system	**O_2/N_2**	**CO_2/N_2**	**CO_2/CH_4**
M4	0.94	0.86	0.64
M5	2.1	9.5	6.1

Obviously, non-coated membranes show high permeances and low permselectivities. The Permeances are 3 to 5 orders of magnitude higher compared to all other membranes in this publication. Additionally, they are not differing by orders of magnitude, which leads to a poor separation effect. This indicates laminar flow or Knudsen diffusion occurring through those membranes. Especially, the permselectivities of non-coated membranes made from NBP and 2M-THF show Knudsen diffusional behavior. This means, a separation effect is occurring, but it's depended on the molecular weight of penetrating species. For calculating the separation effect via Knudsen diffusion, the following equation (8) is used:

$$S_{i,j} = \sqrt{\frac{M_i}{M_j}} \quad (7)$$

Using equation (7), permselectivities by Knudsen diffusion for gas pairs O_2/N_2, CO_2/N_2 and CO_2/CH_4 are 0.94, 0.80 and 0.60, respectively. Small varieties between calculated and obtained Knudsen permselectivities arise from not uniformly sized pores within the membrane. Therefore, non-coated membranes made from NBP and 2M-THF as THF and DMAc replacement are not suitable for gas separation applications but might be interesting as ultrafiltration membranes.

Membranes prepared from NBP and CPME show just for N_2 and CH_4 higher permeances, resulting in poor separation effect. Permeances of those membranes are not reaching those of neat PDMS membranes. PDMS shows permeances two orders of magnitude higher than membranes prepared from NBP and CPME. Nevertheless, the permselectivity is equal to the separation performance of neat PDMS. This means, membranes prepared from NBP and CPME reveal defects not able to separate gases. The flux remains low, since the number of defects is low in PSU membranes resulting in low gas flux and gas separation performance of PDMS membranes. These findings indicate that the combination of NBP and CPME is not suitable for gas separation membranes as well.

 doi:10.20944/preprints202404.2010.v1

Cross-sections of membranes where both harmful solvents were replaced show partially sponge-like membrane structures. The top layer of those membranes is porous as results from gas permeation measurements indicated before. Beneath the porous separation layer voids occurred. In contrast to membranes where just THF was replaced, voids are not occurring over the whole cross-section of those membranes (see Figure 4). Additionally, the voids are not drop-shaped but more finger-like structures. Beneath the void filled part of those membranes a sponge-like structure occurred. Especially, in membranes made from NBP and CPME a layer without structure is to be seen in the cross-section. In the lower left end of Figure 5 (a) it can be clearly seen that even this layer is porous.

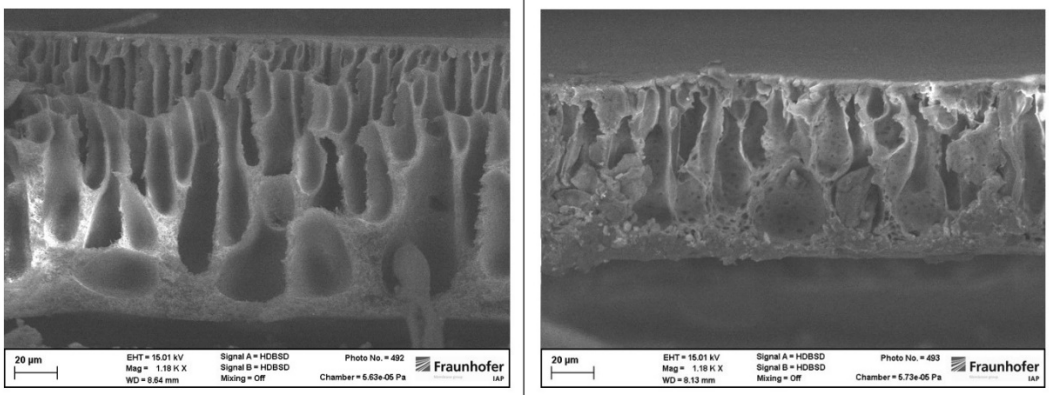

(a) (b)

Figure 4. (a) Cross-section of a membrane prepared from NBP and DMAc. (b) Cross-section of a membrane prepared from 2M-THF and DMAc.

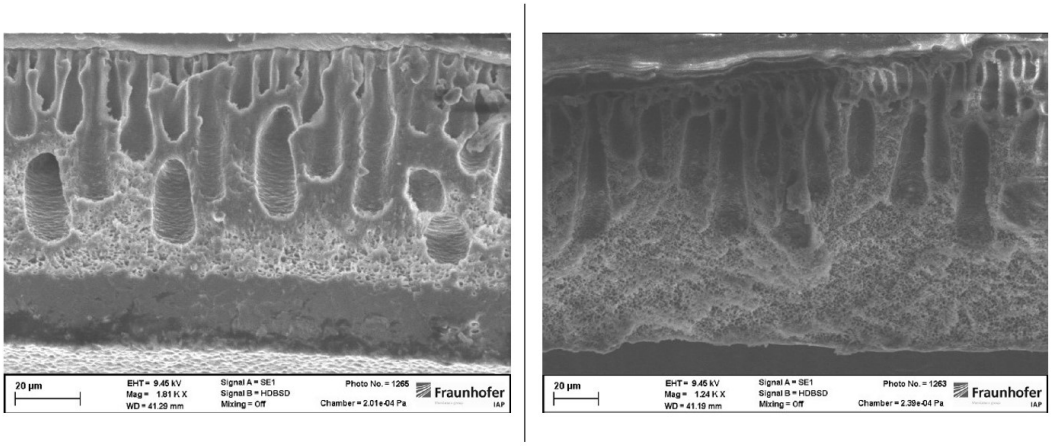

(a) (b)

Figure 5. (a) Cross-section of a PSU membrane prepared from NBP and CPME. (b) Cross-section of a PSU membrane prepared from NBP and 2M-THF.

3.3. Variation of Precipitation Bath Temperature

All membrane structures obtained by greener solvents reveal cross-sections with void filled structures that are not as pressure stable as sponge-like structures. Since void formation is caused by faster diffusion rates of water compared to organic solvents during precipitation an easy way for suppressing void formation is to vary the precipitation bath temperature. Higher temperatures can facilitate the diffusion of organic solvents from the protomembrane into the precipitation medium, suppressing void formation. Cooling the precipitation bath can cause slower exchange and therefore slower penetration of water from the precipitation bath into the protomembrane. Both approaches are examined in this study.

 doi:10.20944/preprints202404.2010.v1

Since membranes where both solvents were replaced by greener alternatives revealed a defective separation layer, for this test series membranes with just a THF replacement were tested. The choice was 2M-THF because fabrication and gas separation performance were closest to those of the standard recipe membranes. Additionally, the voids formed in membranes with 2M-THF as THF alternative were larger and drop-like shaped resulting in a less mechanical stable membrane compared to membranes with NBP as THF alternative. Therefore, changes in the membrane structure are more significant in membranes made from 2M-THF compared to those made from NBP.

3.3.1. Lower Temperature of the Precipitation Bath

The first approach was to lower the temperature of the precipitation bath. The temperature was set to just over 0 °C, so that the water in the precipitation bath just remains liquid. In this case water penetration from the precipitation bath into the protomembrane should be lowered in a way that the formation of voids is suppressed.

After producing PSU membranes at precipitation bath temperatures of 0 °C, membranes with an apparently smoother surface, fewer unevenness and fewer macroscopic defects were fabricated. The precipitation time had to be increased to 15 minutes due to insufficient precipitation after 4 minutes. Insufficient precipitation means that the amount of solvent in membranes after 4 minutes of precipitation was too high. As a result, membranes redissolved when left to dry. This can be explained by the slower solvent exchange at lower precipitation bath temperatures due to lower diffusion of both water and organic solvents. 15 minutes was empirically found to be the shortest time for sufficient precipitation. Gas permeation properties of membranes precipitated at lower temperatures are shown in Table 10.

Table 10. Membrane made from 2M-THF as THF alternative and precipitated at 0 °C.

Permeance [mL(STP)/(cm²·min·bar)]			
O_2	N_2	CO_2	CH_4
$2.71 \cdot 10^{-4}$	$4.26 \cdot 10^{-5}$	$1.69 \cdot 10^{-3}$	$4.76 \cdot 10^{-5}$

Table 11. Membrane made from 2M-THF as THF alternative and precipitated at 0 °C.

O_2/N_2	**CO_2/N_2**	**CO_2/CH_4**
6.4	39.8	35.7

Permeances and separation performance remain at values shown in Tables 6 and 7, when precipitation was carried out at room temperature. The difference in permeances is in the range of 1.85 – 9.47 %, where the largest changes are with nitrogen (+6.57 %) and carbon dioxide (+9.47 %). The smallest change in permeance shows oxygen (+1.85 %). The differences in permeances reveal that these changes are due to the membrane. This means, precipitation at lower temperatures lead to changes on a molecular level of the membranes resulting in changes of the fractional free volume. Since all permeances increased it is considered that due to slower solvent exchange there was more time for the polymer chains to relax during precipitation resulting in an increased fractional free volume.

However, permselectivities of gas pairs CO_2/N_2 and CO_2/CH_4 show an opposite trend. The permselectivities are slightly increased compared to membranes precipitated at room temperature. These small changes can occur when permeances a varying from measurement to measurement and are lying in the range of type c uncertainty of measurement for our setup. This is also the explanation why those permselectivities increased but the permselectivity of the gas pair O_2/N_2 slightly decreased. In contrast to permeances and permselectivities the structure of membranes precipitated at 0 °C changed clearly.

The structure shown in Figure 6 is a clear indicator for slower solvent exchange during precipitation. As mentioned before, lower temperatures of the precipitation bath cause lower diffusion of water molecules into the protomembrane during precipitation. Therefore, non-solidified

 doi:10.20944/preprints202404.2010.v1

polymer is becoming a gel before it is pushed aside from penetrating water, resulting in a more sponge-like structure beneath a thicker separation layer. Additionally, the sponge-like structure leads to a decreased thickness of the membranes. The thickness is reduced by a factor of 2 – 3 compared to membranes precipitated at higher temperatures. Nevertheless, the thicker separation layer is not showing higher permselectivities compared to membranes precipitated at room temperature, as shown Tables 5 and 7. This indicates that thinner separation layers obtained from other recipes in this study are mostly free of defects.

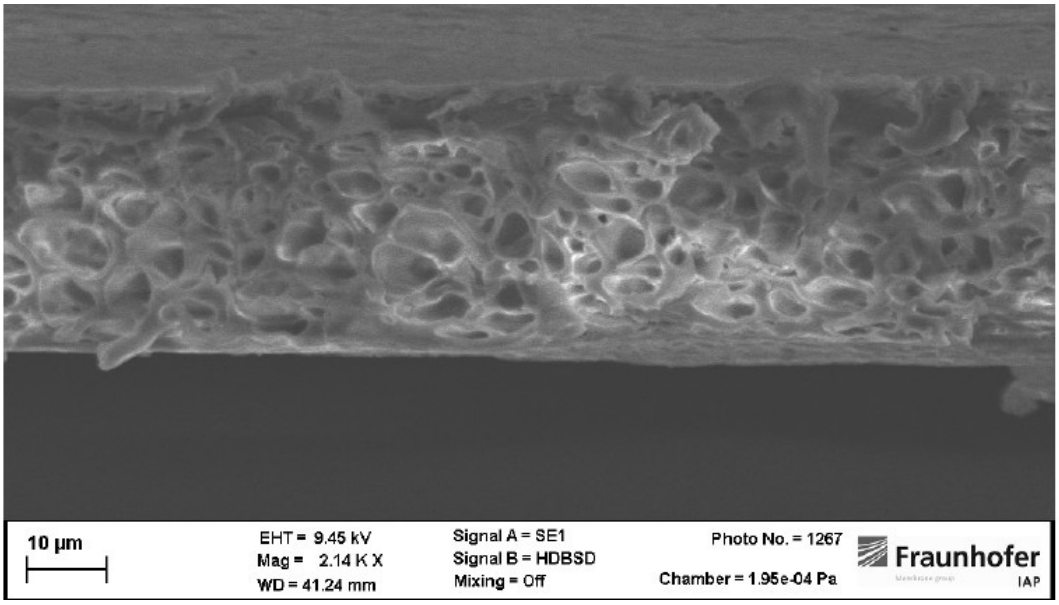

Figure 6. Cross-section of a PSU membrane prepared from 2M-THF as THF alternative precipitated at 0 °C.

Precipitation at 0 °C shows to be an easy way of controlling the morphology of membranes where THF is replaced by 2M-THF. In this way a more mechanically stable membrane structure can be obtained. Additionally, membrane performance regarding permeances and permselectivities is not changed significantly. It has also been noticed that permselectivities are just varying within uncertainty of measurement compared to membranes precipitated at room temperature.

3.3.2. Higher Temperature of the Precipitation Bath

In this approach a higher precipitation bath temperature was chosen. This should have an effect of organic solvents diffusing out of the protomembrane into the precipitation bath whilst precipitation. The temperature was set to 60 °C to facilitate diffusion of organic solvents.

After setting the precipitation bath temperature to 60 °C, macroscopic defects were noticed on the membrane surface, which increased in both number and size compared to membranes prepared at room temperature. Sampling therefore was more difficult. Nevertheless, samples without defects could be taken and successfully been measured. Results are shown in Tables 12 and 13.

Table 12. Membrane made from 2M-THF as THF alternative and precipitated at 60 °C.

Permeance [mL(STP)/(cm²·min·bar)]			
O_2	N_2	CO_2	CH_4
$2.06 \cdot 10^{-3}$	$1.07 \cdot 10^{-3}$	$1.12 \cdot 10^{-2}$	$3.51 \cdot 10^{-3}$

 doi:10.20944/preprints202404.2010.v1

Table 13. Membrane made from 2M-THF as THF alternative and precipitated at 60 °C.

O_2/N_2	CO_2/N_2	CO_2/CH_4
2.2	10.5	3.2

Permeances of membranes precipitated at 60 °C are 1 – 2 orders of magnitude above those of membranes precipitated at room temperature. This indicates that the separation layer is defective or porous. However, PDMS shows permeances even one order of magnitude higher than those shown in Table 12, indicating that no larger defects occurred in PSU membranes but pores. permselectivities reveal that only the PDMS protective layer had a separation effect. In this case, PSU membranes were not effectively separating gases but being a support for PDMS reducing the gas flux of neat PDMS. The morphology of membranes precipitated at 60 °C is depicted in Figure 7.

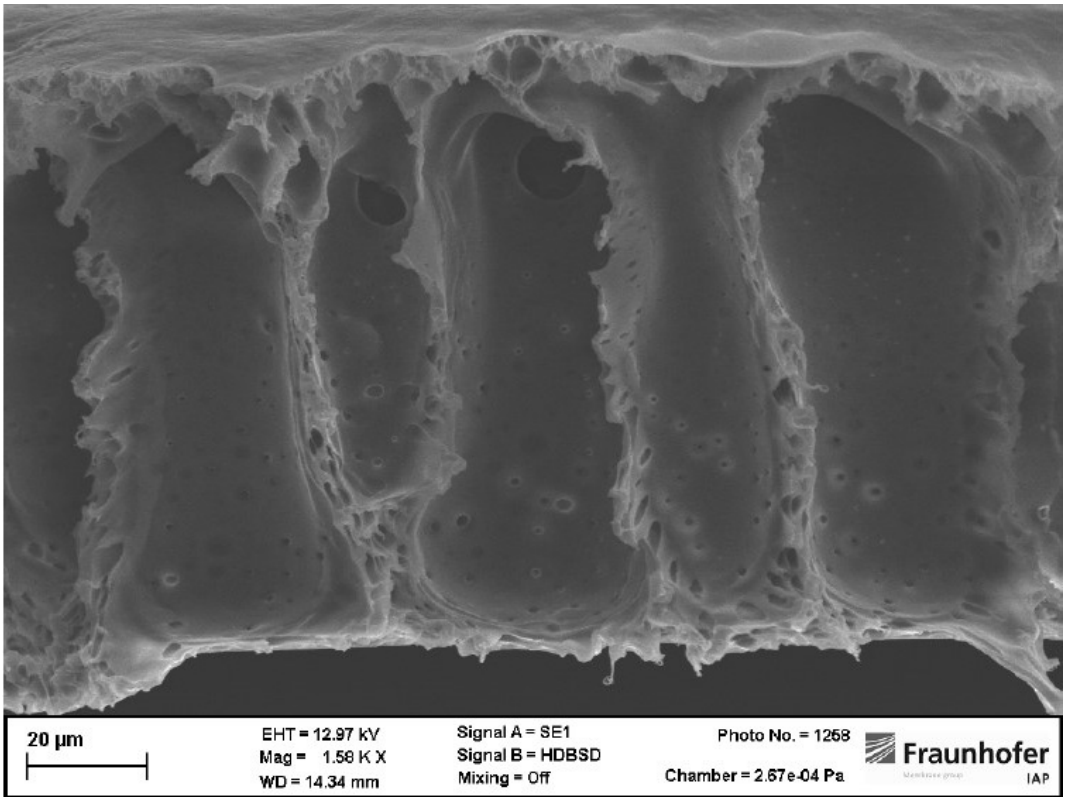

Figure 7. Cross-section of a PSU membrane prepared from 2M-THF as THF alternative precipitated at 60 °C.

Figure 7 shows that higher precipitation bath temperatures are facilitating the diffusion of water molecules more strongly than the diffusion of organic solvent molecules during precipitation. This goes in line with findings of other research groups. The effect of stronger penetrating water is seen by larger voids in membranes precipitated at 60 °C compared to membranes precipitated at room temperature or 0 °C. Because of the increased temperature water is faster penetrating the protomembrane during precipitation. As a result, non-solidified polymer gel is pushed aside by penetrating water forming walls between the voids. These larger voids are leading to a less mechanically stable membrane. However, in case of a defect free separation layer this structure would also lead to higher permeances compared to membranes prepared at lower precipitation bath temperatures. This is because gas transport away from the separation layer is much less hindered in membranes with large voids below the separation layer.

As seen in gas permeation measurements the separation layer is porous, which is also caused by penetrating water during precipitation. This indicates that the osmotic pressure of water between precipitation bath and protomembrane is too high for forming a pore free gas separation layer.

 doi:10.20944/preprints202404.2010.v1

3.4. Comparison with Literature

To evaluate the data acquired in this study, it is compared with literature data. An overview is given in Table 14.

Table 14. Separation performance of polysulfone membranes.

	Permselectivity [–]		
Membrane	**O_2/N_2**	**CO_2/N_2**	**CO_2/CH_4**
M1	5.7	32.7	28.8
M2	6.7	38.3	34.0
M4	0.94	0.86	0.64
M5	2.1	9.5	6.1
M2 (0 °C)[a]	6.4	39.8	35.7
PSf [49]	-	-	36.4
PSF-DMF[50][b]	5.5	13.5	38.3
PSF-THF[50] [b]	5.6	10.5	29.7
PSF-DMAc[50] [b]	6.1	10.4	29.1
PSU[51][c]	-	-	23.12
PSF[52][d]	-	-	31.65
PSF[53][e]	-	-	22.0
PDMS[47] [e]	2.0	7.0	3.2

[a] precipitated at 0°C. [b]measured at 10 bar & 35 °C. [c]measured at 5 bar. [d]measured at 8 bar & 25 °C. [e]measured at 35 °C.

It can be clearly seen that precipitation temperature is not affecting the separation performance of PSU membranes prepared 2M-THF as THF alternative. This is a good indicator for reproducibility and a low value of defects in the gas separation layer. Moreover, membranes of this study show high separation performance for the gas pair CO_2/N_2 compared to membranes from Maghami et al. It has to be mentioned that there is a variety of measuring conditions since no standard is set for gas permeation measurements. Additionally, it is not standardized if permeability or permeances are given in literature. This makes it very difficult to compare data. This is also why in Table 14 just unitless permselectivities are shown. Even this table is difficult for comparison, because applied pressure and temperature while measurement have a large influence on the separation performance of membranes in general. As a rule of thumb, lower pressures and temperatures are leading to higher separation performance but to lower permeances.

4. Conclusions

In this study, the existing membrane-solvent system PSU/THF/DMAc was to be improved in terms of its sustainability without deteriorating the gas separation properties of PSU membranes. The morphology of those membranes should then be adjusted by varying selected process parameters to obtain a mechanically more stable membrane. the membrane produced were assessed for their gas separation performance using the time-lag method. Visual representation was done by SEM imaging.

The results of this study showed that in this system just THF can be replaced to maintain gas separation properties. Additionally, just 2 of 3 selected solvents, namely 2M-THF and NBP, were able to successfully replace THF without changing the recipe. It has to be mentioned that with NBP as THF alternative precipitation times had to be changed from 4 min to at least 20 min to have complete solvent exchange. Whenever THF was replaced, the sponge-like structure of PSU membranes changed to a void filled, mechanically less stable membrane morphology. Replacing DMAc in all tests lead to void filled, porous membranes not capable of separating gases effectively.

For the first time in this study, we could show by simply varying the temperature of the precipitation bath that void formation could be suppressed. This means that even the with the more sustainable solvent 2M-THF mechanically stable sponge-like membrane morphology can be obtained.

 doi:10.20944/preprints202404.2010.v1

Future studies should deal with replacing DMAc and in the end also methanol to eliminate all toxic solvents with more sustainable solvents. This approach would lead to mechanically stable PSU membranes for gas separation made from sustainable solvents, which is in times of climate change and stricter regulations more attractive for membrane producers and applicants.

Author Contributions: Conceptualization, S.K. and K.H.; methodology, S.K.; validation, S.K., K.H. and M.T.; resources, K.H.; data curation, S.K.; writing—original draft preparation, S.K.; writing—review and editing, K.H. and M.T.; visualization, K.H.; supervision, M.T.; project administration, S.K.; funding acquisition, S.K. All authors have read and agreed to the published version of the manuscript.

Funding: This research was funded by Fachagentur Nachwachsende Rohstoffe e.V. (FNR), grant number 2220NR156A. The APC was funded by Fraunhofer Society.

Data Availability Statement: The data presented in this study are available on request from the corresponding author due to restrictions in Fraunhofer Society about data security.

Acknowledgments: In this section, you can acknowledge any support given which is not covered by the author contribution or funding sections. This may include administrative and technical support, or donations in kind (e.g., materials used for experiments).

Conflicts of Interest: The authors declare no conflict of interest. The funders had no role in the design of the study, in the collection, analyses, or interpretation of data, in the writing of the manuscript or in the decision to publish the results.

References

1. Mulder, M. *Basic Principles of Membrane Technology;* Kluwer Academic Publishers, 1996, ISBN 0-7923-4247-X.
2. Kahrs, C.; Schwellenbach, J. Membrane formation via non-solvent induced phase separation using sustainable solvents: A comparative study. *Polymer* **2020**, *186*, 122071, doi:10.1016/j.polymer.2019.122071.
3. Yang, H.-C.; Wu, Q.-Y.; Liang, H.-Q.-.; Wan, L.-S.; Xu, Z.-K. *J Polym Sci B Polym Phys* **2013**, *51*, 1438–1447.
4. Lalia, B.S.; Kochkodan, V.; Hashaikeh, R.; Hilal, N. A review on membrane fabrication: Structure, properties and performance relationship. *Desalination* **2013**, *326*, 77–95, doi:10.1016/j.desal.2013.06.016.
5. Liu, M.; Chen, D.-G.; Xu, Z.-L.; Wei, Y.-M.; Tong, M. Effects of nucleating agents on the morphologies and performances of poly(vinylidene fluoride) microporous membranes via thermally induced phase separation. *J of Applied Polymer Sci* **2013**, *128*, 836–844, doi:10.1002/app.38234.
6. Strathmann, H.; Kock, K. The Formation Mechanism of Phase Inversion Membarnes. *Desalination* **1977**, *21*, 241–255.
7. Figoli, A.; Marino, T.; Simone, S.; Di Nicolò, E.; Li, X.-M.; He, T.; Tornaghi, S.; Drioli, E. Towards non-toxic solvents for membrane preparation: a review. *Green Chem.* **2014**, *16*, 4034, doi:10.1039/C4GC00613E.
8. Marino, T.; Galiano, F.; Molino, A.; Figoli, A. New frontiers in sustainable membrane preparation: Cyrene™ as green bioderived solvent. *Journal of Membrane Science* **2019**, *580*, 224–234, doi:10.1016/j.memsci.2019.03.034.
9. Kim, D.; Salazar, O.R.; Nunes, S.P. Membrane manufacture for peptide separation. *Green Chem.* **2016**, *18*, 5151–5159, doi:10.1039/C6GC01259K.
10. Razali, M.; Kim, J.F.; Attfield, M.; Budd, P.M.; Drioli, E.; Lee, Y.M.; Szekely, G. Sustainable wastewater treatment and recycling in membrane manufacturing. *Green Chem.* **2015**, *17*, 5196–5205, doi:10.1039/C5GC01937K.
11. Wang, Q.; Li, N.; Bolto, B.; Hoang, M.; Xie, Z. Desalination by pervaporation: A review. *Desalination* **2016**, *387*, 46–60, doi:10.1016/j.desal.2016.02.036.
12. Russo, F.; Galiano, F.; Pedace, F.; Aricò, F.; Figoli, A. Dimethyl Isosorbide As a Green Solvent for Sustainable Ultrafiltration and Microfiltration Membrane Preparation. *ACS Sustainable Chem. Eng.* **2020**, *8*, 659–668, doi:10.1021/acssuschemeng.9b06496.
13. Capello, C.; Fischer, U.; Hungerbühler, K. What is a green solvent? A comprehensive framework for the environmental assessment of solvents. *Green Chem.* **2007**, *9*, 927, doi:10.1039/b617536h.
14. Amelio, A.; Genduso, G.; Vreysen, S.; Luis, P.; van der Bruggen, B. Guidelines based on life cycle assessment for solvent selection during the process design and evaluation of treatment alternatives. *Green Chem* **2014**, *16*, 3045–3063, doi:10.1039/C3GC42513D.

15. Xia, B.; Ding, T.; Xiao, J. Life cycle assessment of concrete structures with reuse and recycling strategies: A novel framework and case study. *Waste Manag.* **2020**, *105*, 268–278, doi:10.1016/j.wasman.2020.02.015.
16. Lawler, W.; Bradford-Hartke, Z.; Cran, M.J.; Duke, M.; Leslie, G.; Ladewig, B.P.; Le-Clech, P. Towards new opportunities for reuse, recycling and disposal of used reverse osmosis membranes. *Desalination* **2012**, *299*, 103–112, doi:10.1016/j.desal.2012.05.030.
17. Kim, D.; Nunes, S.P. Green solvents for membrane manufacture: Recent trends and perspectives. *Current Opinion in Green and Sustainable Chemistry* **2021**, *28*, 100427, doi:10.1016/j.cogsc.2020.100427.
18. Kim, J.F. Recent Progress on Improving the Sustainability of Membrane Fabrication. *Journal of Membarne Science & Research* **2020**, *6*, 241–250.
19. Jaekel, E.E.; Kluge, S.; Tröger-Müller, S.; Tutuş, M.; Filonenko, S. Tunable Gas Permeation Behavior in Self-Standing Cellulose Nanocrystal-Based Membranes. *ACS Sustainable Chem. Eng.* **2022**, *10*, 12895–12905, doi:10.1021/acssuschemeng.2c04806.
20. Nelson, W.M. *Green Solvents for Chemistry: Perspectives and Practice;* Oxford University Press: New York, 2003, ISBN 9780195157369.
21. Jessop, P.G. Searching for green solvents. *Green Chem.* **2011**, *13*, 1391, doi:10.1039/c0gc00797h.
22. Marino, T.; Blasi, E.; Tornaghi, S.; Di Nicolò, E.; Figoli, A. Polyethersulfone membranes prepared with Rhodiasolv®Polarclean as water soluble green solvent. *Journal of Membrane Science* **2018**, *549*, 192–204, doi:10.1016/j.memsci.2017.12.007.
23. Wang, H.H.; Jung, J.T.; Kim, J.F.; Kim, S.; Drioli, E.; Lee, Y.M. A novel green solvent alternative for polymeric membrane preparation via nonsolvent-induced phase separation (NIPS). *Journal of Membrane Science* **2019**, *574*, 44–54, doi:10.1016/j.memsci.2018.12.051.
24. Wang, H.H.; Jung, J.T.; Kim, J.F.; Kim, S.; Drioli, E.; Lee, Y.M. A novel green solvent alternative for polymeric membrane preparation via nonsolvent-induced phase separation (NIPS). *Journal of Membrane Science* **2019**, *574*, 44–54, doi:10.1016/j.memsci.2018.12.051.
25. Tsehaye, M.T.; Wang, J.; Zhu, J.; Velizarov, S.; van der Bruggen, B. Development and characterization of polyethersulfone-based nanofiltration membrane with stability to hydrogen peroxide. *Journal of Membrane Science* **2018**, *550*, 462–469, doi:10.1016/j.memsci.2018.01.022.
26. Evenepoel, N.; Wen, S.; Tilahun Tsehaye, M.; van der Bruggen, B. Potential of DMSO as greener solvent for PES ultra- and nanofiltration membrane preparation. *J of Applied Polymer Sci* **2018**, *135*, doi:10.1002/app.46494.
27. Marino, T.; Galiano, F.; Simone, S.; Figoli, A. DMSO EVOL™ as novel non-toxic solvent for polyethersulfone membrane preparation. *Environ. Sci. Pollut. Res. Int.* **2019**, *26*, 14774–14785, doi:10.1007/s11356-018-3575-9.
28. Rasool, M.A.; Vankelecom, I.F.J. Use of γ-valerolactone and glycerol derivatives as bio-based renewable solvents for membrane preparation. *Green Chem.* **2019**, *21*, 1054–1064, doi:10.1039/C8GC03652G.
29. Bisz, E.; Koston, M.; Szostak, M. N -Butylpyrrolidone (NBP) as a non-toxic substitute for NMP in iron-catalyzed C(sp 2)–C(sp 3) cross-coupling of aryl chlorides. *Green Chem.* **2021**, *23*, 7515–7521, doi:10.1039/D1GC02377B.
30. Jiang, X.; Yong, W.F.; Gao, J.; Shao, D.-D.; Sun, S.-P. Understanding the role of substrates on thin film composite membranes: A green solvent approach with TamiSolve® NxG. *Journal of Membrane Science* **2021**, *635*, 119530, doi:10.1016/j.memsci.2021.119530.
31. Henderson, R.K.; Jiménez-González, C.; Constable, D.J.C.; Alston, S.R.; Inglis, G.G.A.; Fisher, G.; Sherwood, J.; Binks, S.P.; Curzons, A.D. Expanding GSK's solvent selection guide – embedding sustainability into solvent selection starting at medicinal chemistry. *Green Chem.* **2011**, *13*, 854, doi:10.1039/c0gc00918k.
32. Lee, W.J.; Goh, P.S.; Lau, W.J.; Ismail, A.F.; Hilal, N. Green Approaches for Sustainable Development of Liquid Separation Membrane. *Membranes (Basel)* **2021**, *11*, doi:10.3390/membranes11040235.
33. Kluge, S.; Kose, T.; Tutuş, M. Tuning the Morphology and Gas Separation Properties of Polysulfone Membranes. *Membranes (Basel)* **2022**, *12*, doi:10.3390/membranes12070654.
34. Oxley, A.; Livingston, A.G. Effect of polymer molecular weight on the long-term process stability of crosslinked polybenzimidazole organic solvent nanofiltration (OSN) membranes. *Journal of Membrane Science* **2024**, *689*, 122149, doi:10.1016/j.memsci.2023.122149.
35. Rinku, T.; Guillen-Burrieza, E.; Arafat, H.A. Pore structure control of PVDF membranes using a 2-stage coagulation bath phase inversion process for application in membrane distillation (MD). *Journal of Membrane Science* **2014**, *452*, 470–480.
36. *Membarne Technology in the Chemical Industry;* Nunes, S.P.; Peinemann, K.-V., Eds., 2nd ed.; WILEY-VCH: Weinheim, 2006, ISBN 3527313427.
37. Kluge, S.; Weiß, M. Herstellung und Charakterisierung von Polysulfon-Membranen für die Gastrennung. *Chemie Ingenieur Technik* **2022**, *94*, 585–593, doi:10.1002/cite.202100013.
38. Broens, L.; Altena, F.W.; Smolders, C.A.; Koenhen, D.M. Asymmetric membrane Structures as a Result of Phase Separation Phenomena. *Desalination* **1980**, *32*, 33–45.

39. Lau, W.W.Y.; Guiver, M.D.; Matsuura, T. Phase separation in polysulfone/solvent/water and polyethersulfone/solvent/water systems. *Journal of Membrane Science* **1991**, *59*, 219–227.
40. Subramanian, S.; Heydweiller, J.C.; Stern, S.A. Dual-mode sorption kinetics of gases in glassy polymers. *J Polym Sci B Polym Phys* **1989**, *27*, 1209–1220, doi:10.1002/polb.1989.090270603.
41. Smit, E.; Mulder, M.H.V.; Smolders, C.A.; Karrenbeld, H.; van Eerden, J.; Feil, D. Modelling of the diffusion of carbon dioxide in polyimide matrices by computer simulation. *Journal of Membrane Science* **1992**, *73*, 247-257.
42. Pfromm, P.H.; Pinnau, I.; Koros, W.J. Gas transport through integral-asymmetric membranes: A comparison to isotropic film transport properties. *J of Applied Polymer Sci* **1993**, *48*, 2161–2171, doi:10.1002/app.1993.070481210.
43. Pinnau, I.; Hellums, M.W.; Koros, W.J. Gas transport through homogeneous and asymmetric polyestercarbonate membranes. *Polymer* **1991**, *32*, 2612–2617.
44. Graham, T. XVIII. On the absorption and dialytic separation of gases by colloid septa. *Phil. Trans. R. Soc. Lond.* **1866**, *156*, 399–439.
45. ISO. Plastics - Film and sheeting - Determination of gas-transmission-rate: Part 1: Differential-pressure method, 2007, 83.140.10 (ISO 15105-1:2007). Available online: https://www.iso.org/standard/41677.html.
46. Kesting, R.E. The solvent size effect: Solvents and solvent complexes viewed as transient templates which control free volume in the skins of integrally-skinned phase inversion membranes. *Journal of Polymer Science: Part C: Polymer Letters* **1989**, *27*, 187–190.
47. Merkel, T.C.; Bondar, V.I.; Nagai, K.; Freeman, B.D.; Pinnau, I. Gas sorption, diffusion, and permeation in poly(dimethylsiloxane). *Journal of Polymer Sciance: Part B: Polymer Physics* **2000**, *38*, 415–434.
48. Guillen, G.R.; Ramon, G.Z.; Kavehpour, H.P.; Kaner, R.B.; Hoek, E.M. Direct microscopic observation of membrane formation by nonsolvent induced phase separation. *Journal of Membrane Science* **2013**, *431*, 212–220, doi:10.1016/j.memsci.2012.12.031.
49. Moradihamedani, P.; Ibrahim, N.A.; Yunus, W.M.Z.W.; Yusof, N.A. Preparation and characterization of symmetric and asymmetric pure polysulfone membranes for CO 2 and CH 4 separation. *Polymer Engineering & Sci* **2014**, *54*, 1686–1694, doi:10.1002/pen.23706.
50. Maghami, S.; Sadeghi, M.; Baghersad, S.; Zornoza, B. Influence of solvent, Lewis acid–base complex, and nanoparticles on the morphology and gas separation properties of polysulfone membranes. *Polymer Engineering & Sci* **2021**, *61*, 1931–1942, doi:10.1002/pen.25708.
51. Adewole, J.K.; Ahmad, A.L.; Ismail, S.; Leo, C.P.; Sultan, A.S. Comparative studies on the effects of casting solvent on physico-chemical and gas transport properties of dense polysulfone membrane used for CO 2 /CH 4 separation. *J of Applied Polymer Sci* **2015**, *132*, doi:10.1002/app.42205.
52. Aroon, M.A.; Ismail, A.F.; Montazer-Rahmati, M.M.; Matsuura, T. Morphology and permeation properties of polysulfone membranes for gas separation: Effects of non-solvent additives and co-solvent. *Separation and Purification Technology* **2010**, *72*, 194–202, doi:10.1016/j.seppur.2010.02.009.
53. McHattie, J. S., Koros, W. J.; Paul, D.R. Gas transport properties od polysulphones: 2. Effect of bisphenol connector groups. *Polymer* **1991**, *32*.